Science
AAAS

Epigenetic Temporal Control of Mouse Hox Genes in Vivo

Natalia Soshnikova, *et al.*

Science **324**, 1320 (2009);
DOI: 10.1126/science.1171468

Science (print ISSN 0036-8075; online ISSN 1095-9203) is published weekly, except the last week in December, by the American Association for the Advancement of Science, 1200 New York Avenue NW, Washington, DC 20005.

Reed warblers distinguish cuckoos from other nest enemies (*22*) and specifically adjust cuckoo mobbing to local parasitism risk (*4*). The specificity of social learning observed here provides evidence that mobbing is a phenotypically plastic trait, adaptive in the context of brood parasitism. We suggest that naïve individuals may learn from bolder birds or from those who, by chance, observed a cuckoo depredate or parasitize their nest. Further experiments are needed to test whether social learning leads only to a change in the perception of parasitism risk or also may involve the refining of a template for cuckoo recognition, akin to the genetic predispositions that guide learning in other contexts (*13*).

Social learning could trigger a marked increase in host defenses; by focusing on neighbors' responses to adult cuckoos, focal pairs not only increase cuckoo mobbing as a front line of defense (*4*) but are also alerted to increased vigilance (*11*) and egg rejection (*5*, *10*). Therefore, our results support the hypothesis that rapid changes in host defenses (*14*, *16*) may reflect social transmission of responses to adult cuckoos as nest enemies. Social learning has implications for the coevolutionary trajectories of brood parasites and hosts because it promotes phenotypic plasticity that can drive or impede genetic evolution (*25*). Furthermore, by influencing how rapidly hosts lose or gain defenses, social learning may affect the population dynamics of both brood parasites and hosts (*26*).

References and Notes

1. C. Darwin, *On the Origin of Species* (Murray, London, 1859).
2. S. I. Rothstein, S. K. Robinson, Eds., *Parasitic Birds and Their Hosts: Studies in Coevolution* (Oxford Univ. Press, Oxford, 1998).
3. N. B. Davies, *Cuckoos, Cowbirds and Other Cheats* (Poyser, London, 2000).
4. J. A. Welbergen, N. B. Davies, *Curr. Biol.* **19**, 235 (2009).
5. N. B. Davies, M. de L. Brooke, *Anim. Behav.* **36**, 262 (1988).
6. A. Lotem *et al.*, *Anim. Behav.* **49**, 1185 (1995).
7. N. B. Davies *et al.*, *Proc. R. Soc. London Ser. B* **263**, 925 (1996).
8. I. J. Øien *et al.*, *J. Anim. Ecol.* **65**, 147 (1996).
9. A. K. Lindholm, *J. Anim. Ecol.* **68**, 293 (1999).
10. A. Moksnes *et al.*, *Ibis* **142**, 247 (2000).
11. N. B. Davies *et al.*, *Anim. Behav.* **65**, 285 (2003).
12. M. de L. Brooke *et al.*, *Proc. R. Soc. London Ser. B* **265**, 1277 (1998).
13. A. S. Griffin, *Learn. Behav.* **32**, 131 (2004).
14. K. Hale, J. V. Briskie, *J. Avian Biol.* **38**, 198 (2007).
15. R. F. Maloney, I. G. MacLean, *Anim. Behav.* **50**, 1193 (1995).
16. H. Nakamura *et al.*, in *Parasitic Birds and Their Hosts: Studies in Coevolution*, S. I. Rothstein, S. K. Robinson, Eds. (Oxford Univ. Press, Oxford, 1998), pp. 94–112.
17. N. B. Davies, J. A. Welbergen, *Proc. R. Soc. London Ser. B* **275**, 1817 (2008).
18. R. Boyd, P. J. Richerson, *Lect. Math Life Sci.* **20**, 1 (1989).
19. W. Hoppitt, K. N. Laland, *Adv. Stud. Behav.* **38**, 105 (2008).
20. E. Curio *et al.*, *Science* **202**, 899 (1978).
21. See supporting material on *Science* Online for methods and additional text and data.
22. J. A. Welbergen, N. B. Davies, *Anim. Behav.* **76**, 811 (2008).
23. These tests included 5/11 that mobbed during the baseline trial, 5/7 that did not mob during the baseline trial but did so after social learning, and 4/6 that retained a nonmobbing response throughout.
24. M. Cook, S. Mineka, *J. Abnorm. Psychol.* **98**, 448 (1989).
25. T. D. Price *et al.*, *Proc. R. Soc. London Ser. B* **270**, 1433 (2003).
26. F. Takasu *et al.*, *Am. Nat.* **142**, 819 (1993).

27. We thank the Natural Environment Research Council; the National Trust, C. Thorne, and the Wicken Fen Group; English Nature; and M. Brooke, J. Davies, R. Kilner, O. Krüger, and the Behavioural Ecology Group at Cambridge.

Supporting Online Material

www.sciencemag.org/cgi/content/full/324/5932/1318/DC1
Materials and Methods
SOM Text
Fig. S1
References

12 February 2009; accepted 20 April 2009
10.1126/science.1172227

Epigenetic Temporal Control of Mouse *Hox* Genes in Vivo

Natalia Soshnikova[1] and Denis Duboule[1,2]*

During vertebrate development, the temporal control of *Hox* gene transcriptional activation follows the genomic order of the genes within the *Hox* clusters. Although it is recognized that this "*Hox* clock" serves to coordinate body patterning, the underlying mechanism remains elusive. We have shown that successive *Hox* gene activation in the mouse embryo is closely associated with a directional transition in chromatin status, as judged by the dynamic progression of transcription-competent modifications: Increases in activation marks correspond to decreases in repressive marks. Furthermore, using a mouse in which a *Hox* cluster was split into two pieces, we document the necessity to maintain a clustered organization to properly implement this process. These results suggest that chromatin modifications are important parameters in the temporal regulation of this gene family.

Hox genes, which are generally arranged in clusters at genomic loci, are essential for patterning the anterior to posterior animal body axis (*1*–*3*). In vertebrates, these genes are activated in a time sequence that follows their physical order within the cluster, a process referred to as temporal collinearity (*4*). This property is observed in animals developing their trunk via a rostral to caudal time sequence, yet the underlying molecular mechanism is elusive (*5*, *6*). A progressive transition in chromatin state was hypothesized (*7*, *8*), whereby an initially repressed configuration becomes open for transcription. The subsequent observation of chromatin decondensation at these loci when transcription is induced supported this hypothesis (*9*).

Hox genes are repressed by Polycomb group (PcG) proteins (*10*). Mutation of *PcG* genes induces ectopic *Hox* expression and results in posterior homeotic transformations (*11*, *12*). PcG proteins form large complexes with histone-modifying activities; for example, Polycomb Repressive Complex 2 (PRC2) trimethylates histone H3 at lysine 27 (H3K27me3) (*13*–*16*), an essential modification for long-term repression of target genes. In contrast, *Trithorax* group (TrxG) proteins antagonize *PcG* proteins and activate target gene expression (*10*). TRX complexes trimethylate histone H3 at lysine 4 (H3K4me3), a mark generally associated with active transcription (*17*). Genome-wide studies of both H3K27me3 and H3K4me3 modifications in embryonic stem cells (ESC) and other cultured cells have revealed specific profiles during the maintenance phase of *Hox* gene expression in vitro (*18*–*21*). We looked at the in vivo dynamics of chromatin marks during the sequential activation of *Hoxd* genes in developing murine tail buds.

We dissected out mouse tail buds during late somitogenesis when the last *Hox* genes become transcribed (*22*) and performed expression profiling at E8.5 (embryonic day 8.5), E9.0, and E9.5 (Fig. 1A) using tiling arrays covering 2 Mb of DNA containing the *HoxD* cluster. This highly syntenic region (*23*) also contains four ubiquitously expressed genes, *Atp5g3*, *Lnp*, *Mtx2*, and *Hnrpa3*, and two gene deserts (fig. S1). Transcription of *Hoxd1* to *Hoxd9* was active at all three time points (Fig. 1B), reflecting the onset of *Hox* gene transcription during early gastrulation. However, transcriptional progression was observed for more posterior genes, with *Hoxd10* and *Hoxd11* transcribed at E9.0 (Fig. 1B), whereas by E9.5 transcriptional activity had spread over *Hoxd12*, *Hoxd13*, and the nearby neighbor gene *Evx2* (Fig. 1B). Low transcript levels were detected for *Hoxd13* before activation of *Hoxd10* (Fig. 1B, arrow).

We mapped the sites occupied by RNA polymerase II using chromatin immunoprecipitation combined with hybridization on tiling array (ChIP-chip) (Fig. 1B and fig. S1). The Pol II profile corresponded to transcribed regions; whereas virtually no Pol II was scored centromeric to *Hoxd10* at E8.5, signals were detected for both *Hoxd10* and *Hoxd11* at E9.0. At E9.5, the whole centromeric part of the cluster was fully occupied by Pol II (Fig. 1B), indicating that it was recruited in a collinear manner too. In agreement with transcript profiling, a weak Pol II binding was scored at the *Hoxd13* locus at E8.5. Similarly, high levels of H3K9/K14 acetylation (AcH3) were found in

[1]National Research Centre Frontiers in Genetics, Department of Zoology and Animal Biology, University of Geneva, Sciences III, Quai Ernest-Ansermet 30, 1211 Geneva 4, Switzerland. [2]National Research Centre Frontiers in Genetics, School of Life Sciences, Federal Institute of Technology (EPFL), Lausanne, Switzerland.

*To whom correspondence should be addressed. E-mail: Denis.Duboule@unige.ch; Denis.Duboule@epfl.ch

E8.5 tail buds, covering from *Hoxd1* to *Hoxd9* (Fig. 1B). However, AcH3 marks were also scored over the silenced *Hoxd10* and *Hoxd11* (Fig. 1B, arrowheads). Along with the transcriptional activation of these two genes, the levels of AcH3 were expanded to cover the entire gene cluster by day 9.5, matching both the presence of Pol II and the robust transcription of the *Hoxd10* to *Hoxd13* interval. As for *Hox* genes, AcH3 modification appeared at the *Evx2* locus before Pol II binding was scored, consistent with a role for this modification in transcriptional initiation (*17*).

We next investigated the status of both H3K27 and H3K4 trimethylation. H3K27me3 levels were assessed in E8.5 and E9.5 tail buds and in ESC. In ESC, consistent with previous studies (*19*, *20*), H3K27me3 marks, associated with transcriptional repression, covered the entire gene cluster (Fig. 2). Accordingly, transcription of *Hoxd* genes was not detected in these cells (Fig. 2, RNA). During collinear activation in tail buds, a complete loss of H3K27me3 mark was progressively observed over the telomeric part of the cluster, initially from *Hoxd1* to *Hoxd4* at E8.5 and subsequently extending until *Hoxd11* at E9.5 (Fig. 2). Because H3K27me3 disappeared upon gene activation, we conclude that tail bud cells that do not express any *Hox* gene do not implement this repression. H3K27me3 marks slightly overlapped with transcriptionally active regions, for example, over the *Hoxd11-Hoxd12* loci at E9.5 (Fig. 2 and fig. S2), likely illustrating some temporal heterogeneity in the activation of *Hoxd* genes within neighboring cells. Also, samples may have included mixtures of cells expressing and cells not expressing a particular *Hox* gene because of the anterior-posterior extent of the dissected domains. Finally, the H3K27me3 signals were higher over the silenced part of the *Hox* gene cluster in E8.5 tail bud cells than in ESC, suggesting that a tighter repression is implemented during axial development.

We checked whether this progressive demethylation of H3K27 was paralleled by an increased trimethylation of H3K4. Consistent with previous results (*24*), we scored low levels of H3K4me3 over *HoxD* in ESC, with residual signals on CpG islands (Fig. 2). In E8.5 tail buds, however, H3K4me3 marks drastically increased and covered the telomeric part of the cluster up to both *Hoxd10* and *Hoxd11*, which are still silenced at this time point (Fig. 2). Therefore, as for AcH3, H3K4me3 marks were detected before Pol II binding and prelabeled future sites of transcription. At E9.5, elevated levels of H3K4 trimethylation over the *Hoxd12* and *Hoxd11* loci corresponded to their robust transcriptional activation (Fig. 2). Altogether, temporal collinearity in tail buds corresponds to chromatin dynamics, progressing along the cluster and involving the removal of H3K27me3 marks, the methylation of H3K4, and the acetylation of H3. Transcriptional activation along the gene cluster occurs within a region of transition between H3K27me3 and H3K4me3 marks, a window that shifts with time toward the centromeric extremity of the cluster (fig. S2).

This collinear chromatin dynamic suggests a mechanism whereby modifications would spread from the telomeric extremity of the cluster to the opposite end. We assessed this possibility by using mice where the *HoxD* cluster is split into two pieces, separated by a 3-Mb inversion (*25*) (Fig. 3A). In this configuration, the *Hoxd11* to *Hoxd13* region becomes isolated from the rest of the cluster. This allows a test of whether early establishment and dynamic progression of both H3K27me3 and H3K4me3 marks require an integral gene cluster.

From *Hoxd1* to *Hoxd9*, the mutant (*inv*) transcript profile was as in wild type (Fig. 3B), demonstrating that cis regulations required to initiate transcription of these genes either lie within this segment of the cluster or are telomeric (*26*). However, differences were observed close to the break point. First, *Hoxd10* was transcribed at E8.5, whereas this gene is normally silent at this stage. Second, ectopic antisense transcripts were detected in the small posterior half-cluster (fig. S3A), likely triggered by the new genomic neighborhood. As in wild type, premature *Hoxd13* transcription was scored in *inv* mutants, indicating that this transcriptional activity does not require telomeric-located regulatory sequences controlling other genes of the cluster. This late-occurring leakage in temporal collinearity may reflect the spurious activity of enhancers located nearby and dedicated to strongly activate this gene in subsequent morphological contexts (*27*). In E9.5 *inv* tail buds, neither *Hoxd12* nor *Hoxd11* showed transcriptional increase (fig. S3B). Their expression was slightly elevated between E8.5 and E9.5 but remained very low when compared to the wild-type situation. On the other side of the breakpoint, *Hoxd10* transcription peaked as in wild type, whereas transcripts located upstream of *Hoxd10* and originating from the *Hoxd11* locus were reduced in amount due to the break (fig. S3B).

ChIP-chip analyses of H3K4me3 distribution in E8.5 homozygous *inv* tail buds showed enrichment over the *Hoxd12* to *Hoxd10* region, on both sides of the break point (Fig. 3C), whereas

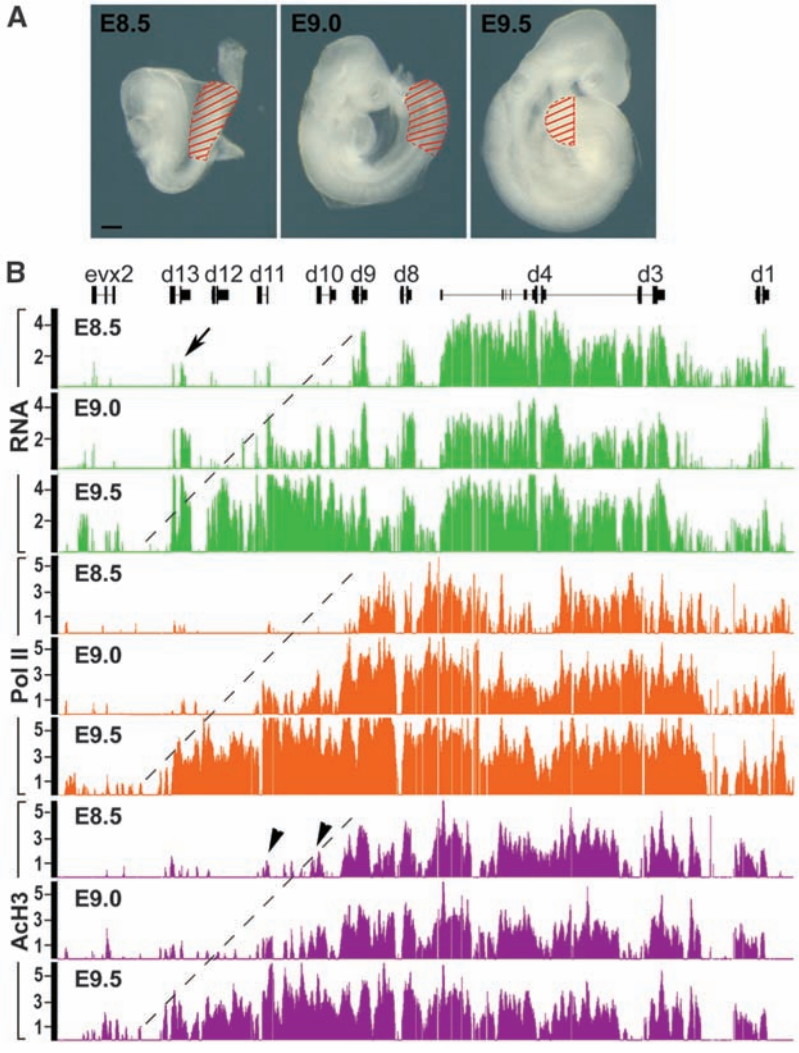

Fig. 1. Collinear activation of *Hoxd* genes during axial development. (**A**) E8.5, E9.0, and E9.5 embryos, with dissected samples indicated in red. Scale bar, 200 μm. (**B**) Transcript profiles on tiling arrays using reverse-transcribed total RNA (green). Bound RNA Pol II (orange) and the AcH3 pattern (magenta) are also displayed for the *HoxD* cluster. The *y* axis indicates the $\log_2$ ratio of cDNA/genomic DNA or ChIP-enriched/input signal intensity.

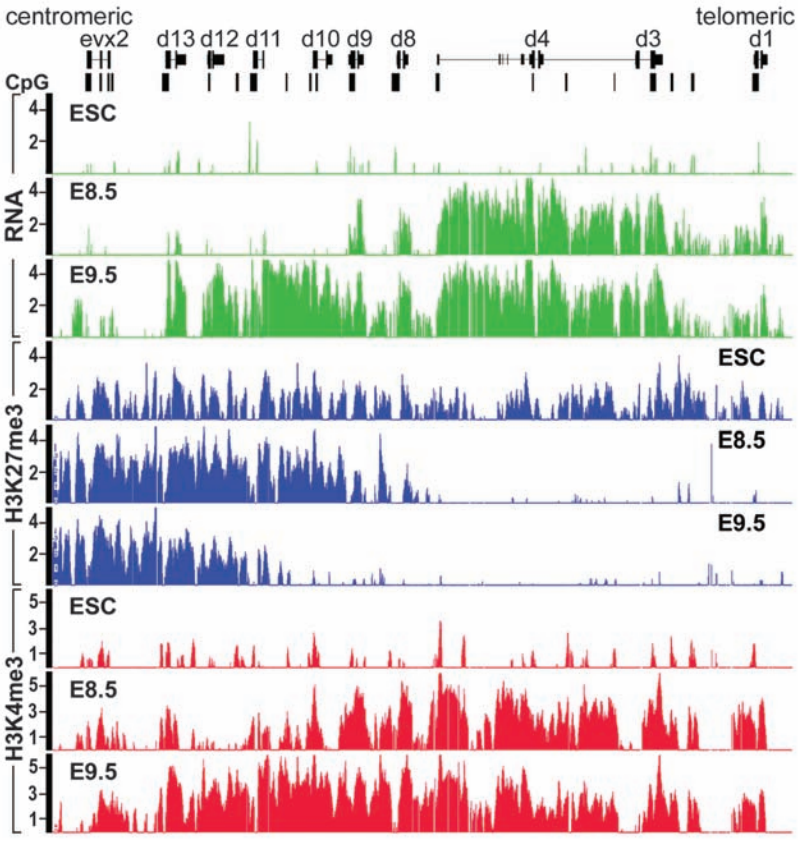

Fig. 2. Chromatin marks during temporal collinearity. Transcriptional activities (green) are shown in ESC and in E8.5 and E9.5 embryos. In ESC, a 120-kb domain is decorated by H3K27me3 (blue), yet at rather low density. In the embryo, H3K27me3 marks progressively retract from the telomeric to the centromeric extremity of the cluster. In addition, levels of H3K27me3 modifications found over silenced genes are higher than in ESC. Low enrichment ($\log_2 \leq 1$) for H3K4me3 (red) marks all CpG islands within *HoxD* in ESC, as opposed to the strong levels ($\log_2 = 4$) detected over *Hoxd1* to *Hoxd9* at E8.5. An increase ($\log_2 \leq 3$) in H3K4me3 marks was also detected at the silenced *Hoxd10*, *Hoxd11*, and *Evx2* loci at this early stage, in the absence of detectable transcripts.

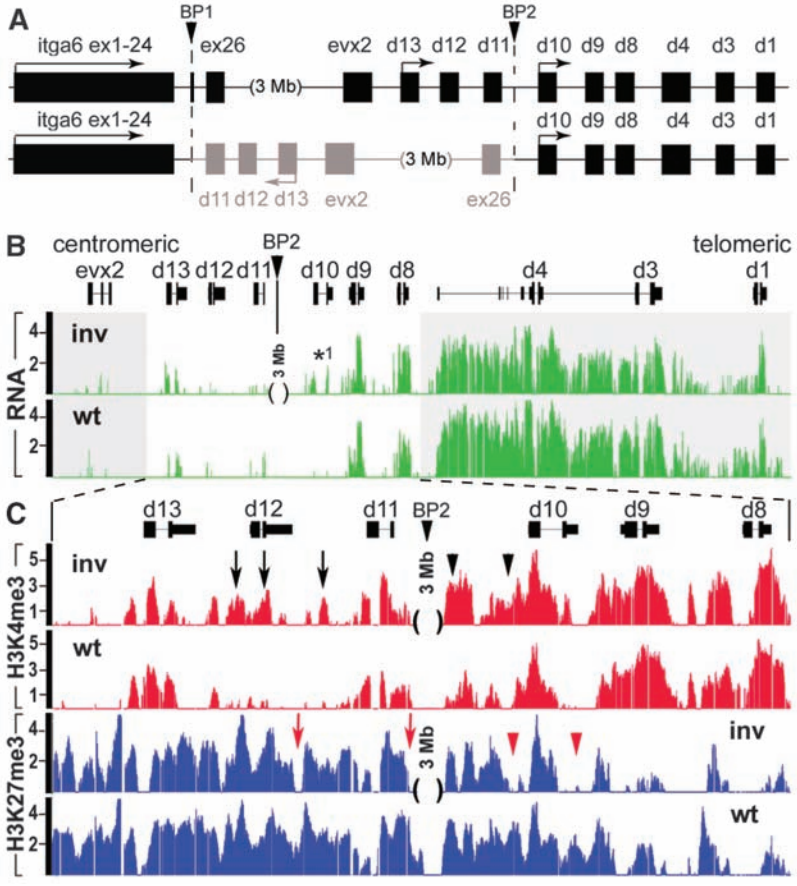

Fig. 3. Transcriptional activation in a split *HoxD* cluster. (**A**) Scheme of the *Integrin-alpha6* (*Itga6*)-*HoxD* inversion (in gray). Dashed lines and arrowheads indicate both breakpoints (BP1 and BP2), either between exons 24 and 26 of *Itga6* or between *Hoxd11* and *Hoxd10*. The inversion positions the centromeric *Hoxd13* to *Hoxd11* DNA segment 3 Mb away from the rest of the cluster. (**B**) Transcript profiles (green) in wild-type (wt) and mutant (*inv*) tail buds at E8.5. Animals with a split cluster activate *Hoxd10* prematurely (E8.5, *1). Only the RNA representing the *Hox*-coding DNA strand is shown (see also fig. S3A). The position of both the break point (BP2) and the 3-Mb interval is indicated. (**C**) Enlargement of the *Hoxd13* to *Hoxd8* region shown in (B) with both H3K4me3 (red) and H3K27me3 (blue) profiles in E8.5 tail buds. Elevated levels of H3K4me3 marks are scored over *Hoxd10*, *Hoxd11*, and *Hoxd12* (black arrows and arrowheads). H3K27me3 marks are reduced at and around the *Hoxd10* locus (red arrowheads) and, to a lesser extent, over *Hoxd11* and *Hoxd12* (red arrows).

the profile from *Hoxd9* to *Hoxd1* was comparable to wild type. The robust gain in H3K4me3 marks over *Hoxd12* was not scored in older wild-type tail buds (fig. S2) and did not match any transcriptional activity, neither for *Hoxd12* nor for *Hoxd11* (Fig. 3B). In this case, both *Hoxd11* and *Hoxd12* were ready to be transcribed (*28*), yet they remained silent because they were moved away from the required enhancer sequence located telomeric to the breakpoint. In contrast, increased H3K4 trimethylation on the other side of the breakpoint (Fig. 3C) matched the premature activation of *Hoxd10*.

The DNA interval decorated by H3K27me3 marks in *inv* mutants was virtually identical to wild type (Fig. 3C), indicating that an integral cluster is not necessary to define the initial extent of the repressive domain; H3K27me3 marks were positioned over posterior genes even though these genes were disconnected from the rest of the cluster, thus ruling out the existence of a spreading mechanism sensu stricto for the implementation of this repression. In addition, the overall density of these marks on both sides of the break point was considerably below the wild-type situation (Fig. 3C). In the posterior half-cluster, H3K27me3 marks were distributed almost as in wild type over *Evx2* and *Hoxd13*, whereas a decrease was scored over the *Hoxd12* to *Hoxd11* intergenic region and 3′ to *Hoxd11* (Fig. 3C). In the anterior half-cluster, a similar reduction was detected at the *Hoxd10* locus, consistent with its premature activation and, to a lesser extent, over *Hoxd9* (Fig. 3C). This weakening in H3K27me3 signal over *Hoxd10* was not observed at the wild-type locus, even in older tail buds (fig. S2). The general decrease in H3K27 trimethylation around the break point suggests that a dense coverage of the *HoxD* cluster by this histone modification requires an intact clustered configuration. Whereas isolated parts of the gene cluster can be trimethylated at H3K27 independently of one another, these various parts may cooperate and synergize to mediate a dense pattern of methylation, potentially through local cis interactions.

These results shed light on the general regulatory strategy implemented by *Hox* gene loci during the earliest steps of mouse trunk development. Unlike in *Drosophila*, mammalian *Hox* gene loci appear refractory to transcription before transcription initiates, as indicated by high levels of H3K27me3 marks covering the *HoxD* locus early on. This likely reflects the necessity to prevent the premature activation of posterior genes at a time when anterior structures are being determined, which would be deleterious to the embryo. During gastrulation, this repression is counteracted by an activity progressing from the telomeric to the centromeric extremity of the cluster, illustrated by both an elevation of H3K4me3 level and the demethylation of H3K27me3. The region of transition between these two states of chromatin corresponds to the dynamic window wherein *Hoxd* genes become transcriptionally active. Alternatively, *Hox* genes could be activated from a persisting pool of nonexpressing stem cells. In this view, the chromatin modifications observed in our samples reflect the average of successive waves of transcriptional activation rather than a dynamic process occurring in the same cells. We do not favor this possibility because such a pool of *Hox*-negative cells would constitute a large fraction of the tissue sample, yet it has never been observed in gastrulating tail buds. Also, the nucleosomes of these stem cells would lack the repressive marks over the *HoxD* cluster, unlike in ESC. Finally, *Hox* genes are activated in cells already expressing more anterior combinations thereof.

We have shown that gene clustering is not necessary for the initial definition of the H3K27me3 landscape. However, clustering is required for a full repression to be consolidated and/or maintained over the cluster, which suggests a synergistic effect due to *Hox* genes' density. Likewise, whereas an integral cluster appears dispensable for selecting the sites of H3K4 trimethylation, gene clustering helps the coordination of this general transition in chromatin status because split clusters displayed premature H3K4me3 marks on either side of the breakpoint. Although the gain of H3K4me3 and the concurrent weakening of H3K27me3 at the mutant *Hoxd10* locus coincided with its early ectopic transcription, similar imbalances at the inverted *Hoxd11* and *Hoxd12* loci did not elicit the same transcriptional response. From this, we conclude that H3K4me3 chromatin modification is necessary but not sufficient for proper *Hox* gene transcriptional control and that remote enhancer sequences must have contributed to the maintenance of clustered organization during animal evolution.

References and Notes

1. D. Duboule, P. Dollé, *EMBO J.* **8**, 1497 (1989).
2. A. Graham, N. Papalopulu, R. Krumlauf, *Cell* **57**, 367 (1989).
3. R. Krumlauf, *Cell* **78**, 191 (1994).
4. J. C. Izpisúa-Belmonte, H. Falkenstein, P. Dollé, A. Renucci, D. Duboule, *EMBO J.* **10**, 2279 (1991).
5. D. Duboule, *Development* **134**, 2549 (2007).
6. M. Kmita, D. Duboule, *Science* **301**, 331 (2003).
7. P. Dollé, J. C. Izpisúa-Belmonte, H. Falkenstein, A. Renucci, D. Duboule, *Nature* **342**, 767 (1989).
8. T. Kondo, D. Duboule, *Cell* **97**, 407 (1999).
9. S. Chambeyron, W. A. Bickmore, *Genes Dev.* **18**, 1119 (2004).
10. Y. B. Schwartz, V. Pirrotta, *Nat. Rev. Genet.* **8**, 9 (2007).
11. J. Simon, A. Chiang, W. Bender, *Development* **114**, 493 (1992).
12. M. van Lohuizen, *Cell. Mol. Life Sci.* **54**, 71 (1998).
13. R. Cao *et al.*, *Science* **298**, 1039 (2002).
14. B. Czermin *et al.*, *Cell* **111**, 185 (2002).
15. A. Kuzmichev, K. Nishioka, H. Erdjument-Bromage, P. Tempst, D. Reinberg, *Genes Dev.* **16**, 2893 (2002).
16. J. Müller *et al.*, *Cell* **111**, 197 (2002).
17. T. Kouzarides, *Cell* **128**, 693 (2007).
18. B. E. Bernstein *et al.*, *Cell* **120**, 169 (2005).
19. A. P. Bracken, N. Dietrich, D. Pasini, K. H. Hansen, K. Helin, *Genes Dev.* **20**, 1123 (2006).
20. T. I. Lee *et al.*, *Cell* **125**, 301 (2006).
21. J. L. Rinn *et al.*, *Cell* **129**, 1311 (2007).
22. J. Deschamps, J. van Nes, *Development* **132**, 2931 (2005).
23. A. P. Lee, E. G. Koh, A. Tay, S. Brenner, B. Venkatesh, *Proc. Natl. Acad. Sci. U.S.A.* **103**, 6994 (2006).
24. B. E. Bernstein *et al.*, *Cell* **125**, 315 (2006).
25. F. Spitz, C. Herkenne, M. A. Morris, D. Duboule, *Nat. Genet.* **37**, 889 (2005).
26. P. Tschopp, B. Tarchini, F. Spitz, J. Zakany, D. Duboule, *PLoS Genet.* **5**, e1000398 (2009).
27. T. Montavon, J. F. Le Garrec, M. Kerszberg, D. Duboule, *Genes Dev.* **22**, 346 (2008).
28. A. S. Chi, B. E. Bernstein, *Science* **323**, 220 (2009).

29. We thank T. Montavon, A. Puglisi, and D. Schübeler for advice; F. Chabaud for cell culture; and P. Descombes and members of the Genomics Platform for their help with tiling arrays. N.S. was supported by a European Molecular Biology Organization long-term fellowship. This work was funded by the University of Geneva, the Federal Institute of Technology in Lausanne, the Swiss National Research Fund, the National Research Center Frontiers in Genetics, and the European Union program Crescendo. Data and analysis are available for download from ArrayExpress (accession E-TABM-677).

Supporting Online Material

www.sciencemag.org/cgi/content/full/324/5932/1320/DC1
Materials and Methods
Figs. S1 to S3
References

27 January 2009; accepted 17 April 2009
10.1126/science.1171468

McsB Is a Protein Arginine Kinase That Phosphorylates and Inhibits the Heat-Shock Regulator CtsR

Jakob Fuhrmann,[1]* Andreas Schmidt,[2]* Silvia Spiess,[3] Anita Lehner,[1] Kürşad Turgay,[4] Karl Mechtler,[1,5] Emmanuelle Charpentier,[3,6] Tim Clausen[1]†

All living organisms face a variety of environmental stresses that cause the misfolding and aggregation of proteins. To eliminate damaged proteins, cells developed highly efficient stress response and protein quality control systems. We performed a biochemical and structural analysis of the bacterial CtsR/McsB stress response. The crystal structure of the CtsR repressor, in complex with DNA, pinpointed key residues important for high-affinity binding to the promoter regions of heat-shock genes. Moreover, biochemical characterization of McsB revealed that McsB specifically phosphorylates arginine residues in the DNA binding domain of CtsR, thereby impairing its function as a repressor of stress response genes. Identification of the CtsR/McsB arginine phospho-switch expands the repertoire of possible protein modifications involved in prokaryotic and eukaryotic transcriptional regulation.

One of the most intensely studied stress-response pathways is the bacterial heat-shock response. In the Gram-positive model organism *Bacillus subtilis*, the heat-shock response is mediated by a complex regulatory network (*1*, *2*) that is under control of at least four